JOURNAL OF MATERIALS SCIENCE 17 (1982) 1389–1397

# Precipitation in non-stoichiometric spinel

W. T. DONLON*, T. E. MITCHELL, A. H. HEUER
*Department of Metallurgy and Materials Science, Case Institute of Technology, Case Western Reserve University, Cleveland, Ohio 44106, USA*

Precipitation in non-stoichiometric spinel ($MgO \cdot 3.5Al_2O_3$) single crystals has been investigated in the temperature range 900 to 1600° C. The formation of a coherent intermediate phase precedes precipitation of the equilibrium $\alpha$–$Al_2O_3$, and the time–temperature–extent of transformation ($T$–$T$–$T$) curve for the formation of this metastable phase has been determined. Nucleation of $\alpha$–$Al_2O_3$ occurs only at free surfaces, presumably because of the large strain energy accompanying the transformation of the anion sublattice from cubic to hexagonal close-packing. The growth rate of $\alpha$–$Al_2O_3$ from the free surfaces follows a linear law and appears similar to the "autocatalytic reaction" found in some metallic alloys. The following orientation relationship between spinel and $\alpha$–$Al_2O_3$ is observed:

$$\langle 10\bar{1}0\rangle_{\alpha\text{-}Al_2O_3} \parallel \langle 110\rangle_{spinel}$$

and

$$(0001)_{\alpha\text{-}Al_2O_3} \parallel \{111\}_{spinel}.$$

## 1. Introduction

Mg–Al spinels ($MgO \cdot nAl_2O_3$, $n > 1$) exist over a wide range of compositions ($n$-values), as shown in Fig. 1 [1]. The charge-compensating defects necessarily present in non-stoichiometric alumina-rich spinels were shown by Jagodzinski and Saalfeld [2] to be cation vacancies. Non-stoichiometric spinel can thus be thought of as a solid solution of stoichiometric spinel with $\gamma$-$Al_2O_3$, i.e. $(MgAl_2O_4)_{1-x} - (Al_{8/3}V_{Al,1/3}O_4)_x$, where $V_{Al}$ is an Al vacancy.

The first systematic study of precipitation reactions in spinel involving both temperature and composition as variables was performed by Saalfeld and Jagodzinski [3]. Their study involved X-ray diffraction and optical microscopy, and they indentified three different stages of precipitation:

(a) formation of a pre-precipitate phase,

(b) formation of a monoclinic intermediate structure of chemical composition $MgO \cdot 16Al_2O_3$ [4], and

(c) the final precipitation of $\alpha$-$Al_2O_3$.

Lewis [5], using transmission electron microscopy (TEM) to study precipitation, indicated two distinct metastable intermediate structures (Type I and Type II), both having monoclinic symmetry but with different morphologies. One of these phases (Type I) was indentical to that observed by Jagodzinski [4] and appeared as thin plates parallel to {3 1 1} matrix planes with the following orientation relationships:

$$\{311\}_{spinel} \parallel (001), \text{ Type } I_{precipitate}$$

and

$$\langle 110\rangle_{spinel} \parallel [010], \text{ Type } I_{precipitate},$$

with unit-cell parameters of $a = 0.931$ nm, $b = 0.564$ nm, $c = 1.210$ nm and $\beta = 119.46°$.

Bansal and Heuer [6] also performed a systematic precipitation study on non-stoichiometric $MgO \cdot 3.5Al_2O_3$ spinel at 850° C and inferred that the pre-precipitates were spherical. The Type I and II intermediate phases precipitated after 4 and 15 h, respectively, and formed preferentially on grown-in sub-boundaries and isolated dislocations; they coarsened on prolonged ageing as the pre-precipitates dissolved. The first equilibrium

*Present address: Ford Motor Company, Scientific Research Laboratory, Dearborn, MI 48121, USA.

0022–2461/82/051389–09$03.58/0  

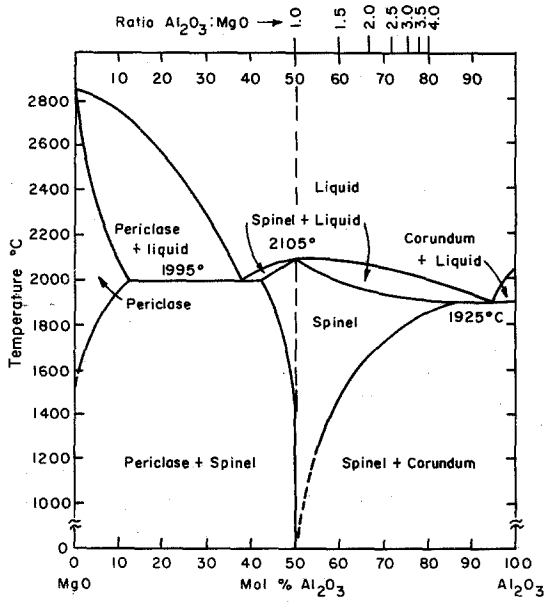


*Figure 1* Phase diagram for the system $MgO–Al_2O_3$ (after Roy *et al.* [1]).

$\alpha$-$Al_2O_3$ phase nucleated after 44 h aging, apparently independent of the existing structures. Upon subsequent annealing, the plates of $\alpha$-$Al_2O_3$ coarsened, although some Type I precipitates could still be observed after 240 h. At 1025° C and after 25 h ageing, only the $\alpha$-$Al_2O_3$ platelets were present.

Doukhan *et al.* [7] also studied precipitation in spinel by beam-heating while the sample was being observed in the electron microscope. These results relate to temperatures (~1800° C) and compositions in the single-phase field; however, evaporation of MgO allowed precipitation to occur. Near the heated zone, three new phases were created, all of which conserve the oxygen sublattice of spinel:

(a) the Type I precipitate with $n \sim 16$, already described,

(b) a tetragonal phase, $\delta_2$, with $n = 3$ and believed to be an equilibrium high-temperature phase in the system, and

(c) a monoclinic phase, $\theta$, with $n = 40$.

None of these previous investigations has systematically studied precipitation in non-stoichiometric spinel over a large range of temperatures. One possibly unrecognised difficulty involved in studying precipitation at high temperatures is the evaporation of MgO from the surface of the specimen. The MgO-depleted surface layer can inhibit further evaporation but more seriously will affect the stoichiometry of the bulk sample. To minimize this undesirable phenomenon, all specimens in this study were aged while packed in MgO powder unless otherwise noted.

The observation of Saalfield and Jagodzinski [3] that $\alpha$-$Al_2O_3$ precipitates preferentially at the surface of the specimen probably indicates that there is a high nucleation barrier for the formation of $\alpha$-$Al_2O_3$. Since this study is concerned primarily with the kinetics of precipitation, the first portion of this paper will describe the phases that form in the interior of single crystals.

## 2. Experimental techniques

Single-crystal boules of non-stoichiometric Mg–Al spinel ($MgO \cdot 3.5Al_2O_3$), grown by the Verneuil process, were obtained from Hrand Djevahirdjian SA, Monthey, Switzerland. Specimens were oriented using the back-reflection Laue technique and cut with a slow-speed saw into parallelepipeds, 3 mm × 3 mm × 7.5 mm, with the long axis of the specimen parallel to a ⟨1 1 1⟩ direction.

Specimens were packed in MgO powder using a cold-mounting press to limit surface evaporation of MgO and were aged in air at 900° C to 1600° C for various times; they were then air-quenched by removing from the furnace. Foils for transmission electron microscopy (TEM) were prepared

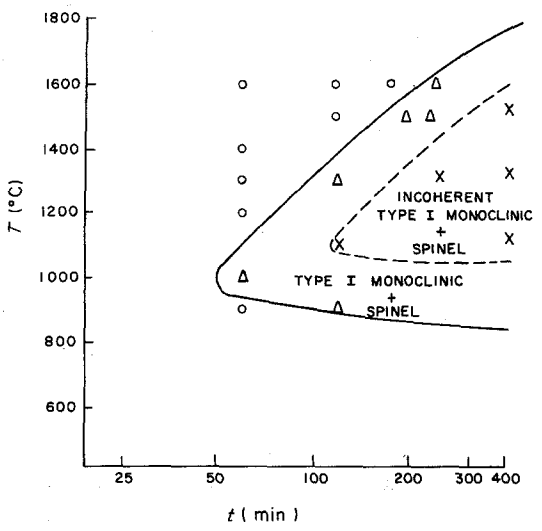


*Figure 2* *T–T–T* curve for the formation of the coherent Type I monoclinic phase and its loss of coherency. The circles, triangles and crosses represent single-phase samples, samples containing coherent precipitates and samples containing incoherent precipitates, respectively.

by cutting and polishing a thin section from the centre of the specimen, followed by ion-bombardment thinning. These foils were then examined using either a Hitachi HU-650 or a Siemens 102 electron microscope.

## 3. Results

### 3.1. Formation of Type I monoclinic particles

At short ageing times, the volume-fraction of precipitates was too small to be detected by conventional X-ray diffraction and TEM was used to identify the phases present and their morphology. A time–temperature–extent of transformation (*T–T–T*) curve for the initial formation of the Type I monoclinic phase was determined and is shown in Fig. 2.

The morphology of this phase varied as ageing proceeded. At the earliest stages of precipitation, the Type I phase exists as very thin plates; in a $[011]$ foil, the traces of the plates are parallel to $\langle 2\bar{1}1\rangle$ (Fig. 3). The narrowness of the plates gives rise to $\langle 111\rangle$ streaking in the diffraction pattern (inset to Fig. 3).

The $\{311\}_{spinel}$ habit plane of the Type I phase found by Lewis was confirmed by the following experiments:

(a) The thin plates of Fig. 3 were tilted so that they were edge-on; this produced streaking along $\langle 311\rangle$.

(b) Coarser particles, such as produced by aging at 1000° C for 1 h, could be tilted so that the habit plane was parallel to the electron beam (see Fig. 4). This orientation was such that a prominent zone-aixs direction in the particle, $[100]$, was parallel to $[\bar{2}33]$ in spinel, thus leading to the identification of $(311)_{spinel}$ as the habit plane.

(c) For a **g** vector of $[04\bar{4}]$ (Fig. 5), no contrast is observed between the precipitate and the matrix, suggesting that $\mathbf{g}\cdot\mathbf{R} = 0$ for this condition, where **R** is the displacement across the precipitate–matrix interface and is parallel to $[311]$.

As ageing proceeds, the volume-fraction of the Type I phase increases as expected, and the particles coarsen. Fig. 6 shows a series of increasingly coarser particles. Many particles contain anti-phase boundaries, as reported by Lewis [5] (Fig. 6b). At this stage of the precipitation reaction, the particles have an irregular ellipsoidal shape, rather than the plate-like morphology shown above (Figs 3 to 5), and dislocations are observed in the precipitate–matrix interface, possibly indicating that coherency has been lost (Fig. 6c). The loss of coherency appears to be associated with the break-up of the long plate-like particles; this (assumed) coherent → incoherent reaction is also plotted in Fig. 2.

No $\alpha$-$Al_2O_3$ was observed in any of the samples whose microstructures are shown in Figs 3 to 6, although for some ageings, $\alpha$-$Al_2O_3$ did precipitate on the surface of the sample. As already noted, this phenomenon was also reported by Saalfeld and Jagodzinski [3]. Bansal and Heuer [6] reported the presence of $\alpha$-$Al_2O_3$ in their sample aged at 1050° C for 25 h. The morphology of what Bansal and Heuer identify as $\alpha$-$Al_2O_3$, however, is identical to that seen in Fig. 7a, which is, in fact, an over-aged Type I precipitate (Fig. 6c is from this same sample); when the ageing treatment used by Bansal and Heuer was repeated, i.e. the samples annealed in air, only incoherent Type I precipitates were observed (Fig. 7b).

### 3.2. Precipitation of $\alpha$-$Al_2O_3$

It is clear from the phase diagram (Fig. 1) that the equilibrium phase mixture for a non-stoichiometric

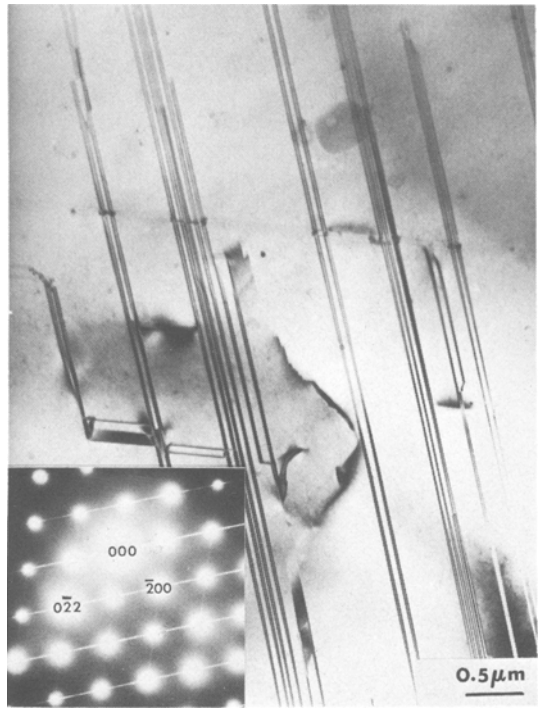


*Figure 3* Bright-field electron micrograph of thin Type I precipitates. The $[011]_{spinel}$ diffraction pattern included as an inset shows that these plates cause streaking in the $\langle 111\rangle$ directions. Sample aged at 1300° C for 2 h in MgO.

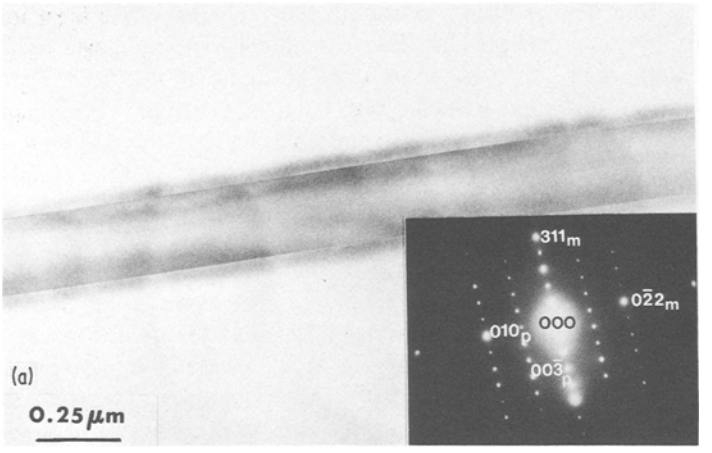


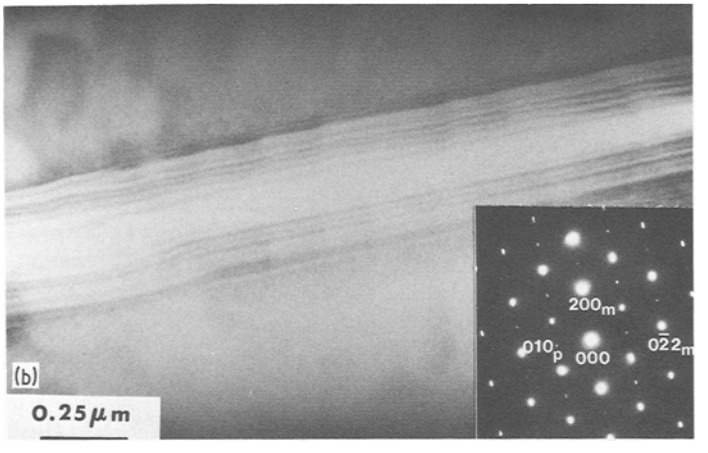


*Figure 4* Bright-field electron micrograph of Type I precipitate (a) viewed edge-on along $[\bar{2}33]_{\text{spinel}}$; (b) viewed along $[011]_{\text{spinel}}$ to show thickness fringes at the interfaces. Specimen aged at 1000° C for 1 h in MgO. The inset diffraction patterns (in which p and m refer to precipitate and matrix, respectively) reveal the following orientation relationships:

$$[\bar{2}33]_{\text{spinel}} \parallel [100]_{\text{Type I}},$$

$$(01\bar{1})_{\text{spinel}} \parallel (010)_{\text{Type I}}$$

and

$$(311)_{\text{spinel}} \parallel (001)_{\text{Type I}}.$$

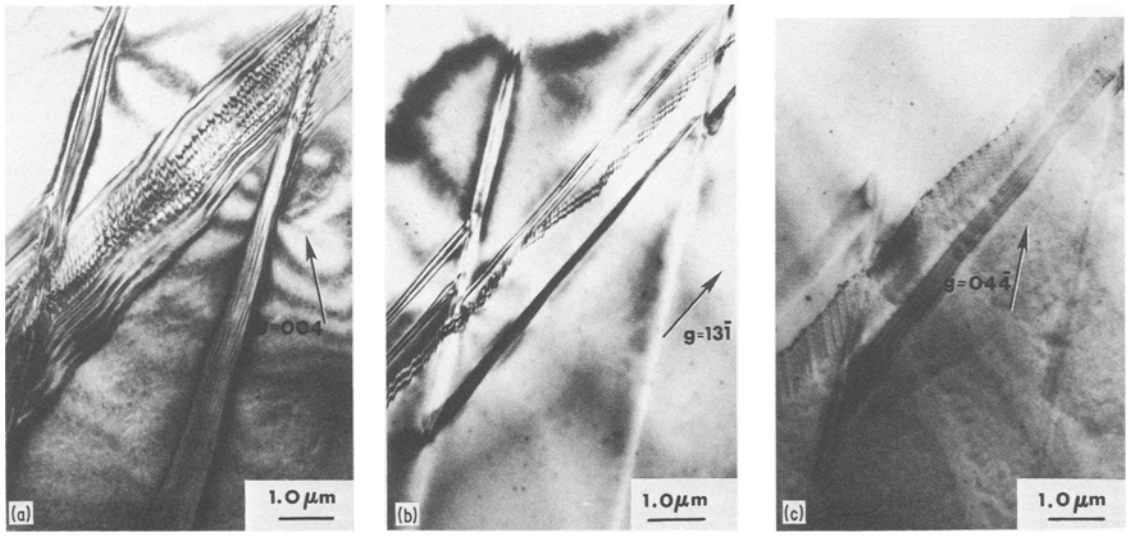


*Figure 5* Bright-field electron micrographs of Type I precipitates formed at 1000° C for 1 h. Imaging with the several g-vectors shown confirms that the habit plane is {311}. Note that $\mathbf{g}\cdot\mathbf{R} = 0$ for two of the precipitates imaged with $\mathbf{g} = 04\bar{4}$.

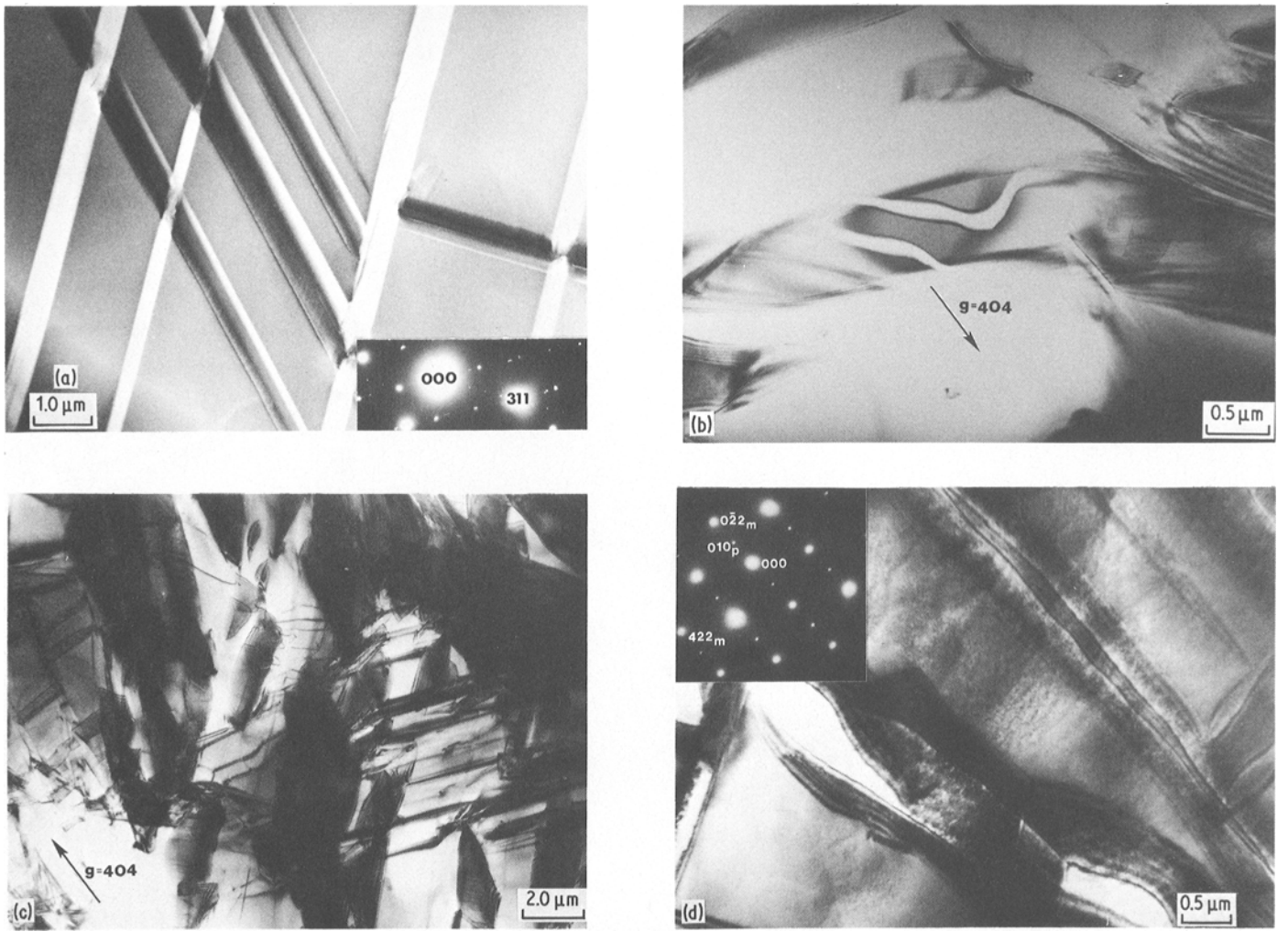


*Figure* 6 Bright-field electron micrographs of coarse Type I particles formed on ageing in MgO: (a) aged for 4 h at 1500° C, (b) aged for 2 h at 1100° C, (c) aged for 1300° C, and (d) aged for 7 h at 1500° C.

$n = 3.5$ spinel at temperatures below ~ 1800° C is spinel plus $\alpha$-$Al_2O_3$. The composition of the product spinel phase varies continuously with decreasing temperature, and does not approach stoichiometry ($n = 1$) until below 1000° C. At intermediate temperatures, e.g., near the nose of the Type I *T–T–T* curve (Fig. 2), this metastable phase forms preferentially. At these temperatures, therefore, the reaction sequence is spinel → spinel + Type I → spinel + $\alpha$-$Al_2O_3$, rather than the direct precipitation of $\alpha$-$Al_2O_3$ from non-stoichiometric spinel.

The $\alpha$-$Al_2O_3$ plates so formed were readily identifiable using either optical microscopy or X-ray diffraction methods, whereas the Type I phase was difficult to detect by these techniques. Portions of the crystal which had precipitated $\alpha$-$Al_2O_3$ appeared white to the naked eye (Fig. 8a) and showed X-ray diffraction peaks of $\alpha$-$Al_2O_3$, while areas containing the Type I phase plus spinel were transparent. The reaction front separating the two-phase (spinel + $\alpha$-$Al_2O_3$) assemblage from the two-phase (spinel + Type I) assemblage was sharp and readily visible by optical microscopy (Fig. 8b and c). As seen in Fig. 8b and c both of which show a {1 1 1} spinel surface, four variants of the $\alpha$-$Al_2O_3$ plate-like precipitates are present as the precipitate forms preferentially with {1 1 1} spinel habit planes [8]. This evidence, combined with electron diffraction analysis (not presented here), leads to the following orientation relationship:

$$\{1\,1\,1\}_{\text{spinel}} \| (0\,0\,0\,1)_{Al_2O_3}$$

and

$$\langle \bar{1}\,1\,0 \rangle_{\text{spinel}} \| \langle 1\,0\,\bar{1}\,0 \rangle_{Al_2O_3}.$$

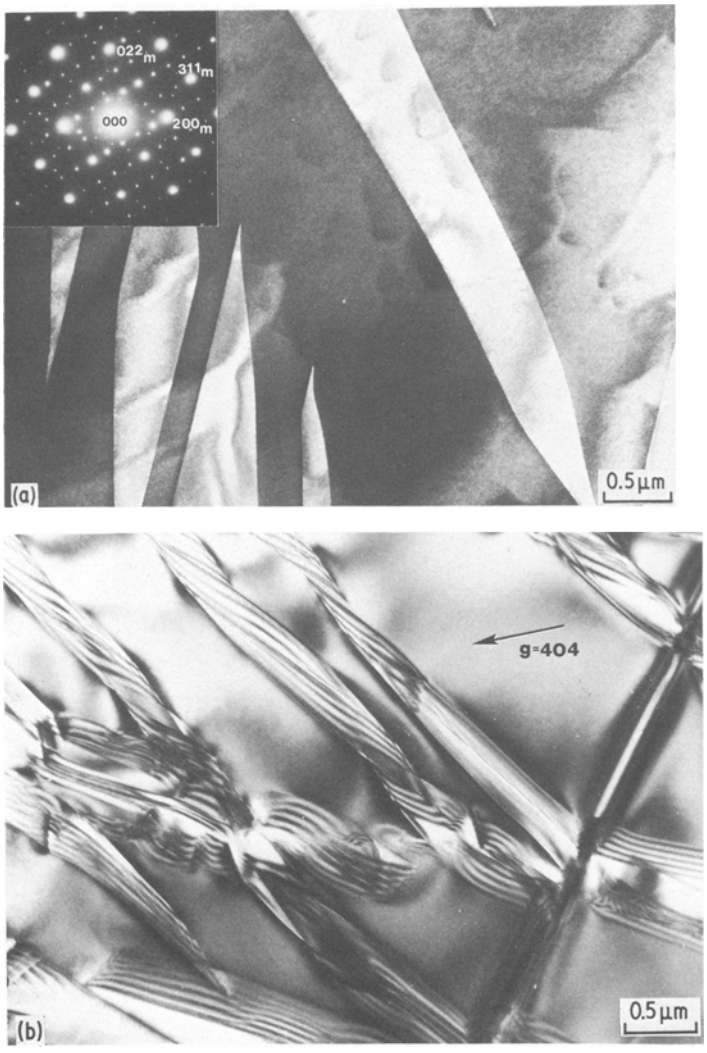


*Figure 7* Bright-field electron micrographs of incoherent Type I monoclinic particles: (a) aged for 4 h at 1300° C in MgO; (b) aged for 25 h in air at 1050° C. See text for further discussion.

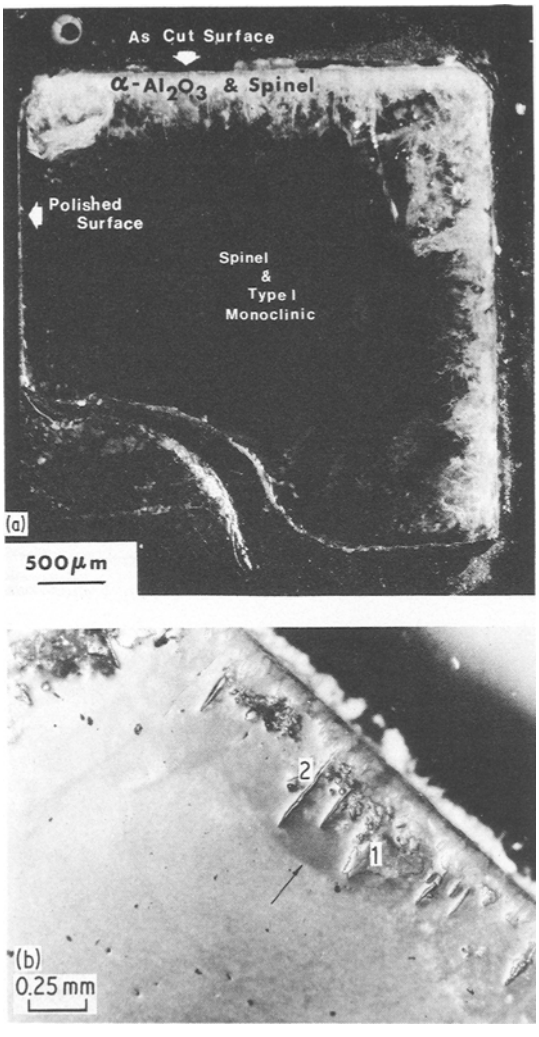


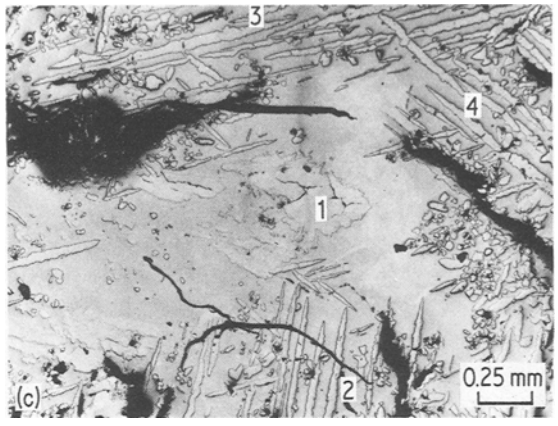


*Figure 8* Optical micrographs (reflected light). (a) Cross-section of a specimen aged for 12 h at 1300° C in MgO, showing $\alpha$-$Al_2O_3$ only on the top and right surfaces, which were unpolished before aging. (b) $(1\,1\,1)_{spinel}$ surface showing early stages of reaction yielding spinel + $\alpha$-$Al_2O_3$. The reaction front (arrowed) is sharp; two of the four $\alpha$-$Al_2O_3$ variants (numbered 1 and 2) are visible in this field of view. (c) $(1\,1\,1)_{spinel}$ surface in an almost completely reacted sample. All four variants are visible.

This orientation relationship is such that the close-packed oxygen planes and directions in the cubic spinel are parallel to the equivalent hexagonal close-packed planes and directions in alumina.

At the reaction front, the Type I phase is being dissolved and $\alpha$-$Al_2O_3$ is precipitating. It appears from Fig. 8 that the reaction product nucleates exclusively on free surfaces. An incubation period for nucleation was noted for well-polished but not for as-cut surfaces; this incubation period was 15 h at 1300° C.

The kinetics of the formation of (spinel + $\alpha$-$Al_2O_3$) was determined from measurements of the phase front (Fig. 8b) and was unmistakably linear (Fig. 9). The incubation period for the polished surface is clearly evident in Fig. 9: note that the slope of the linear curves are identical for the two surface conditions.

Surface evaporation of MgO did affect the extent of the $\alpha$-$Al_2O_3$ layer. A 3 mm thick sample heated for 24 h at 1300° C in air formed $\alpha$-$Al_2O_3$ throughout the entire thickness, while the $\alpha$-$Al_2O_3$ layer of a sample similarly annealed in MgO powder was $350 \pm 200\,\mu m$ thick. Direct precipitation of $\alpha$-$Al_2O_3$ occurred on one occasion. A specimen which had previously been deformed at 1300° C to yield a high dislocation density [9] was aged in argon for 100 min. This ageing allowed an appreciable amount of $\alpha$-$Al_2O_3$ to form; no mestable phase was found.

## 4. Discussion

The initially-formed Type I precipitates have been previously identified by Lewis [5] and precipitation of similar metastable phases in the $MgO \cdot nGa_2O_3$ system have been reported by Bassoul *et al.* [10, 11]. The Type II phase, which was observed by both Lewis [5] and Bansal and Heuer [6], was not observed in this study and probably only forms at lower temperatures. Stubican *et al.* [12] studied precipitation in the $MgO$–$Al_2O_3$–$Cr_2O_3$ system and presented a *T–T–T* curve for both the intermediate and the $\alpha$-$Al_2O_3$ phases which contained a nose near 1500° C. In their investigation, they aged their specimens in a vacuum, and although they reported a small loss of 1 to 2 mole per cent

of $Cr_2O_3$ during the heat treatment, the problem of MgO evaporation was not addressed.

The difficulty of precipitating the equilibrium $\alpha$-$Al_2O_3$ at the temperatures studied here indicates that there is a very high barrier for nucleating this phase in the spinel matrix; precipitation occurs only on free surfaces or on a pre-existing dislocation substructure. This is in contradiction to the work of Bansal and Heuer [6], who thought that randomly orientated $\alpha$-$Al_2O_3$ plates formed in a sample aged for 25 h at 1050° C. Their experiments were repeated with the present specimens but no $\alpha$-$Al_2O_3$ was observed either in the bulk or on the surface of the specimen. Morphologically, some of the precipitates formed during this ageing were identical to those seen by them; however, electron diffraction indicated that these precipitates were the Type I phase.

The large nucleation barrier for the formation of $\alpha$-$Al_2O_3$ implied by our work is thought to result from the transformation of the oxygen sublattice from the cubic close-packing of spinel to the hexagonal close-packing of $\alpha$-$Al_2O_3$. In contrast, the precipitation of the Type I phase only involves cation redistribution (diffusion); the oxygen sublattice is continuous between the particles and the spinel matrix, which are presumably coherent. While this fcc → hcp transformation in close-packed metals, e.g., Co, does not involve much *volume* strain, this is not the case in spinel. For example, at 1300° C, the equilibrium composition of non-stoichiometric spinel is $MgO \cdot 1.8\,Al_2O_3$ and the corresponding lattice parameter is approximately 0.800 nm. There are 32 oxygen atoms per unit cell, and so the volume per oxygen atom in spinel is 0.016 $nm^3$. The corresponding unit cell of $\alpha$-$Al_2O_3$ with $a_0 = 0.4758$ nm and $c_0 = 1.2991$ nm contains 18 oxygen atoms and so the volume per oxygen atom is 0.0141 $nm^3$. There is therefore a 13% volume change on precipitation and it is this large lattice strain that leads to the difficult nucleation of $\alpha$-$Al_2O_3$.

The linear kinetics observed here are typical of the many discontinuous [13] and cellular reactions in metallic systems which give rise to duplex (usually lamellar) reaction products. As the spinel phase appears to be crystallographically continuous across the reaction front (Fig. 8b), the reaction is most like those found in certain iron alloys and termed [14] "autocatalytic", in that "the orientation of the matrix is unchanged by decomposition, there is no grain boundary or other visible defect at the reaction front, and the second phase forms not as lamellae perpendicular to the reaction front but as plates with crystallographic habit planes" [14]. The slope of the curves in Fig. 9 are presumably proportional to some interface diffsution coefficient which governs the dissolution of Type I and the reprecipitation of $\alpha$-$Al_2O_3$. However, we have not applied the standard equations governing such reactions because the lamellar spacings do not seem sufficiently periodic and because of the multiplicity of $\alpha$-$Al_2O_3$ variants formed behind the advancing interface.

## 5. Conclusions

The relative ease of formation and growth of the Type I precipitates from non-stoichiometric spinel must be due to their initial coherency with the spinel lattice. Upon extended ageing, when the

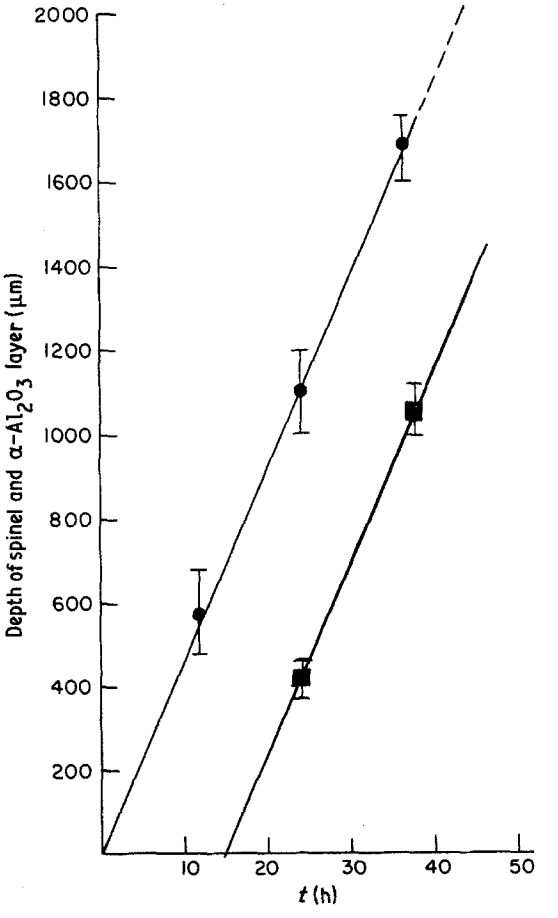


*Figure 9* Depth of precipitated layer plotted against time for samples aged at 1300° C in MgO. Circles are for cut surface, while squares are for polished surface.

formation of $\alpha$-$Al_2O_3$ is suppressed because of the difficulty of nucleation, the Type I precipitates grow and lose coherency during Ostwald ripening.

The difficulty of precipitating $\alpha$-$Al_2O_3$ from spinel has been seriously underestimated in past investigations. Both surface flaws and MgO evaporation enhance the nucleation and growth of the lamellar $\alpha$-$Al_2O_3$ + spinel reaction product. This difficulty of nucleation must be due to the large strain energy associated with the transformation of the oxygen sublattice from the fcc structure of spinel to the hcp structure of $Al_2O_3$. The growth rate is linear and similar to "autocatalytic" reactions found in some metallic systems.


## Acknowledgement

This research was supported by the DOE under Grant No. DEAS0277, ERRO4217.


## References


1. D. M. ROY, R. ROY and E. F. OSBORN, *J. Amer. Ceram. Soc.* **36** (1953) 149.
2. H. JAGODZINSKI and H. SAALFIELD, *Z. Kristallog.* **110** (1958) 197.
3. H. SAALFIELD and H. JAGODZINSKI, *ibid.* **109** (1957) 87.
4. H. JAGODZINSKI, *ibid* **109** (1957) 388.
5. M. H. LEWIS, *Phil. Mag.* **20** (1969) 895.
6. G. K. BANSAL, and A. H. HEUER, *ibid* **29** (1974) 709.
7. N. DOUKHAN, J. C. DOUKHAN and B. ESCAIG, *Mater. Res. Bull.* **11** (1976) 125.
8. A. H. HEUER and T. E. MITCHELL, in "Precipitation Processes in Solids" edited by K. C. Russell and H. T. Aaronson, (Metals Society of the AIME, Warrendale, PA, 1978).
9. W. T. DONLON, PhD Thesis, Case Western Reserve University, Cleveland, Ohio (1981).
10. P. BASSOUL, A. DUBON, A. LEFEBVRE and J. C. GILLES, *Phys. Stat. Solidi* **34** (1976) 125.
11. *Idem, J. Phys.* **38** (1977) C7-80.
12. V. S. STUBICAN, C. GRESKOVICH and H. A. McKINSTRY, *J. Amer. Ceram. Soc.* **52** (1969) 174.
13. D. B. WILLIAMS and E. P. BUTLER, *Int. Met. Rev.* **26** (1981) 153.
14. E. HORNBOGEN, *Met. Trans.* **3** (1972) 2717.



*Received 21 September*
*and accepted 9 October 1981*